Computer Simulation of Chains in Dilute Solution. Crossover from Θ to Good Solvent Behavior

John G. Curro* and Dale W. Schaefer

Sandia Laboratories,† Albuquerque, New Mexico 87185. *Received February 12, 1980*

ABSTRACT: Monte Carlo calculations are reported on isolated chains of various lengths up to 299 units as a function of temperature. The purpose of this investigation is to look for evidence for "thermal blobs" as postulated in the renormalization approach to chain statistics. By calculating the expansion factor for short internal sequences of monomers, we find more expansion than would be predicted from application of the blob theory. This effect is shown to be due to repulsive interactions between the internal sequence of monomers and the rest of the chain. This effect, however, does not influence the exponents predicted by the blob theory for the overall dimensions of the chain. The Monte Carlo simulations are performed by using an extension of the "reptating" sampling technique of Wall, generalized to include an attractive potential.

In this investigation Monte Carlo simulations are performed on an isolated polymer chain as a function of temperature (or equivalently solvent quality). The purpose of this work is to check the validity of the blob concept[1] as a model for the crossover in chain statistics from good to poor solvent behavior.[2]

Monte Carlo calculations have previously been carried out by McCrackin, Mazur, and Guttman.[3,4] These investigators computed the mean square end-to-end distance $\langle r^2 \rangle$ and radius of gyration $\langle s^2 \rangle$ as a function of temperature. The solvent is accounted for by varying the magnitude of the nearest-neighbor attractive energy of a polymer chain on a lattice. It was found that both $\langle r^2 \rangle$ and $\langle s^2 \rangle$ were proportional to N^γ, where N is the number of chain units. Over the range of N studied ($20 \leq N \leq 2000$), the exponent γ varied continuously from $^6/_5$ in a good solvent to 1 at the Θ point. In this investigation, calculations were performed on a simple cubic lattice identical with that of McCrackin et al., but with a sampling procedure similar to that developed by Wall and co-workers.[5] For simplicity, all internal rotational energy states are taken to be equal. Unlike previous investigations, we establish the statistical properties of the internal parts of the chain, as well as the end-to-end distance, by Monte Carlo simulation. This information is used to determine if the "thermal blob" theory can be applied to internal sequences of segments within a chain.

In the simplest form of the blob theory, sequences of m monomers are presumed ideal for $m < N_\tau$, where N_τ is a critical degree of polymerization which defines a blob. The overall chain of N monomers is then represented as a chain of N/N_τ renormalized monomers, or blobs. The temperature dependence of the chain expansion depends entirely on the temperature dependence of N_τ. This theory has been checked by Farnoux[1] et al., who examined the angle dependence of the static structure factor obtained by small-angle neutron scattering. These results indicated that short sequences showed ideal statistics as assumed in the blob theory. The neutron data, however, were necessarily analyzed at large scattering angles where the intensity is low and where background corrections compromise the data.

Computer simulation provides an alternate method to examine short sequences which is not subject to the limitation of neutron scattering. Although simulation is just the real-space analogue of the Farnoux et al. neutron work, simulation is not subject to background problems and also permits analysis of a system with an exactly specified pair potential. In what follows, therefore, we examine the statistical properties of internal sequences and compare the results to blob theory. The results show that the renormalization approach severely underestimates the swelling of short segments.

Monte Carlo Method

A polymer plus solvent system constrained to lattice is equivalent to the polymer molecules alone on the lattice with a nearest-neighbor attractive energy.[3,4,6] This energy ϵ is the difference of the pair interaction between like and unlike species. That is

$$\epsilon = \epsilon_{11} + \epsilon_{00} - 2\epsilon_{10} \tag{1}$$

where ϵ_{11}, ϵ_{00}, and ϵ_{01} are the polymer–polymer, solvent–solvent and solvent–polymer interactions, respectively. McCrackin and co-workers[3,4] have shown that as ϵ changes from 0 to some finite value, the polymer chain contracts in a manner characteristic of the crossover from a good to Θ solvent. This method is used in the present study.

The polymer chain configuration is sampled on the lattice with a "slithering snake" or reptating motion used in simulations by Wall and co-workers.[5] With this sampling method, either end of the chain is moved to an adjacent lattice point and the rest of the chain follows behind in a snakelike fashion. To a good approximation this technique efficiently and uniformly samples configuration space. Although the method is approximate due to "double cul-de-sacs",[5,7] these trapped configurations represent a negligible effect.

In previous applications of the slithering-snake sampling procedure, the chain interactions were hard sphere in nature. In this work we generalize the procedure to include nearest-neighbor attractive potentials, using the Metropolis[8,9] algorithm for accepting new configurations. The procedure consists of the following steps:

1. The chain is initially put in some arbitrary configuration.
2. Either the 1st or Nth segment is moved to a randomly chosen adjacent lattice point with the rest of the chain following behind.
3. If this lattice position is occupied by another chain segment, the chain is moved back to its previous position, and the opposite end of the chain is moved according to step 2.
4. If the energy of the new configuration is less than the energy of the old configuration, the new configuration is accepted, and the same end of the chain is moved according to step 2.
5. If the energy E_2 of the new configuration is greater than the energy E_1 of the previous configuration, then a random number R ($0 \leq R \leq 1$) is chosen. a. If $R < \exp(E_1 - E_2)$, then the new configuration is accepted and the same

† A U.S. Department of Energy facility.

0024-9297/80/2213-1199$01.00/0

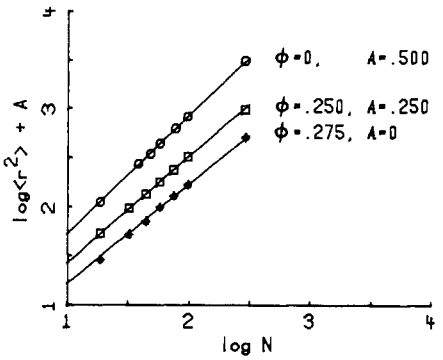

Figure 1. Comparison of the mean square end-to-end distance $\langle r^2 \rangle$ (as a function of chain length N) obtained in this investigation (points) and the work of McCrackin[4] et al. (lines). The results are shown for three different values of solvent quality ϕ (or temperature). For clarity, the ordinate is shifted by an arbitrary constant A shown for each line.

end of the chain is moved according to step 2. b. If $R > \exp(E_1 - E_2)$, then the chain is moved back to the previous configuration and the opposite end of the chain is moved according to step 2.

6. Some observable property of interest X_i is computed for this ith configuration.

Steps 2–6 are repeated a large number of times (M) and the observable quantity of interest is averaged according to

$$\langle X \rangle = M^{-1} \sum_{i=1}^{M} X_i \tag{2}$$

It can be shown[9] that this procedure leads to configurations with a probability proportional to the Boltzmann factor $\exp(-E_i/kT)$ after a large number of iterations.

As a check on the validity of the sampling procedure, we compared our values of mean square end-to-end distance on a simple cubic lattice with the results of McCrackin and co-workers, who used a different Monte Carlo technique. The results are shown in Figure 1 for three values of $\phi = \epsilon/kT$. It can be seen that there is good agreement between the two methods.

Crossover. Comparison of Monte Carlo Results with the Blob Model

A. Blob Model. It is well established that for finite chains in a good solvent, the mean square end-to-end distance $\langle r^2 \rangle$ and the radius of gyration $\langle s^2 \rangle$ are proportional to N^γ, where N is the degree of polymerization and $\gamma \simeq {}^6/_5$. As the temperature is lowered, γ decreases and becomes equal to 1 at the Θ temperature. As indicated above, the blob model accounts for the temperature dependence of $\langle r^2 \rangle$ through a single parameter N_τ, the degree of polymerization of a blob. Since the chain is presumed ideal for sequences less than N_τ, the mean blob radius ξ_τ is given by the random-flight result

$$\xi_\tau^2 = N_\tau a^2 \tag{3}$$

where a is the monomer size. This equation can be improved by using perturbation theory within the blob. The end-to-end distance then follows since the renormalized chain is a sequence of blobs of radius ξ_τ with full excluded volume between blobs. That is

$$\langle r^2 \rangle = \xi_\tau^2 (N/N_\tau)^{6/5} = N_\tau^{-1/5} a^2 N^{6/5} \tag{4}$$

where N/N_τ is the number of blobs in the chain. The expansion factor α follows directly:

$$\alpha^2 = \frac{\langle r^2 \rangle}{Na^2} = \left(\frac{N}{N_\tau} \right)^{1/5} \tag{5}$$

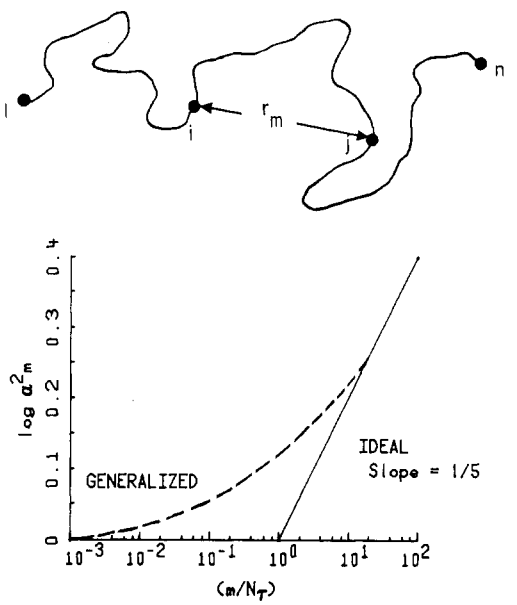

Figure 2. Schematic drawing of a polymer chain showing an internal sequence of $m = j - i$ monomers. Also shown is the representation of the behavior of the internal expansion factor α_m as a function of m. Note an abrupt change in slope (idealized theory) at $m = N_\tau$, where N_τ is the number of monomers per blob. The concave dashed line is the result expected if perturbation theory is assumed to apply inside the blob.

In a good solvent ($T \gg \Theta$) $N_\tau \sim 1$ whereas in a poor solvent ($T \sim \Theta$), $N_\tau \sim N$. Thus, the blob varies from one monomer under good-solvent conditions to the entire chain at the Θ temperature.

B. Monte Carlo Results. The existence of blobs can be established from analysis of the internal chain conformation. Let us define an internal average $\langle r_m^2 \rangle$ which can be evaluated from Monte Carlo calculations. $\langle r_m^2 \rangle$ is defined as the mean square distance of a sequence of m monomer units along the chain (see Figure 2). This average is computed from

$$\langle r_m^2 \rangle = (N - m + 1)^{-1} \sum_{i=1}^{N-m+1} \langle r_{i,i+m}^2 \rangle \tag{6}$$

where $\langle r_{i,i+m}^2 \rangle$ is the mean square distance between points i and $i + m$ on the chain. We can then define an internal expansion factor α_m

$$\alpha_m^2 = \langle r_m^2 \rangle / \langle r_m^2 \rangle_0 \tag{7}$$

where $\langle r_m^2 \rangle_0$ is the value for an ideal chain with no excluded volume ($\langle r_m^2 \rangle_0$ is known exactly for the simple cubic lattice used here[10]). If the blob model is taken literally, then a plot of log α_m^2 vs. log m would be expected to show an abrubt change in behavior from a line of slope zero to a line of slope ${}^1/_5$ at $m = N_\tau$, as shown in Figure 2. If one relaxes the assumptions so that within the blob the average size is given by simple perturbation theory, rather than being completely ideal, then one would expect a gradual change in slope from zero to ${}^1/_5$ with a concave up line shown in Figure 2 (see Appendix). In either case, short sequences should show properties approaching those of a Gaussian chain.

In this investigation we computed α_m^2 from Monte Carlo calculations as a function of m for chains up to 299 units in length. These results are shown in Figure 3 for chains of 299 units. It can be seen that for temperatures above the Θ temperature[4] ($\epsilon/kT < 0.28$), the plot shows a concave down shape. This is opposite to the behavior we would expect on the basis of the blob model. The dashed lines

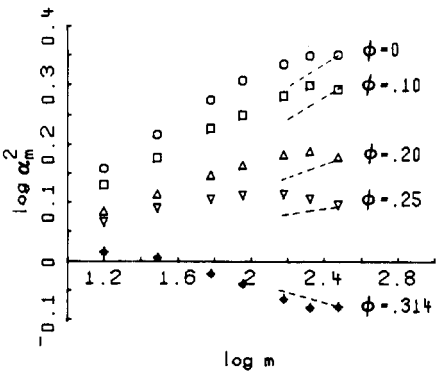

Figure 3. Monte Carlo results (points) for the internal expansion factor α_m as a function of sequence length m for chains of 299 units, at various values of ϕ. The dashed lines represent the end-to-end expansion factors for chains of length m. Note that above the Θ point ($\phi < 0.28$) the internal expansion is greater than the end-to-end distance of the chain having the same number of segments ($m \leq 299$) as the internal sequence length.

shown on this plot are the corresponding end-to-end expansion factors of chains shorter than 299 segments. It can be seen that the Monte Carlo results imply that the internal expansion factor α_m is greater than would be predicted on the basis of the end-to-end distance of a chain of m units. This behavior is apparently due to the interaction of the m internal units in question with the remainder of the chain.

C. Perturbation Theory. In order to explain the internal expansion effect, it is instructive to consider the predictions of perturbation theory applied to the entire chain. Conventional perturbation theory assumes that the interaction potential is completely described by the binary cluster integral v, which is proportional to the monomer's second virial coefficient[2]

$$v = \int [1 - \exp(-w(r)/kT)]\, d\vec{r} \tag{8}$$

where $w(r)$ is the pair potential. For a chain of N units, the internal expansion factor α_m and the end-to-end expansion factor α can be written to first order as[11]

$$\alpha^2 = 1 + \frac{G_3}{N}\left(\frac{3}{2\pi}\right)^{3/2}\left(\frac{v}{a^3}\right) + O\left(\frac{v}{a^3}\right)^2 \tag{9}$$

$$\alpha_m^2 = 1 + \frac{(G_3 + 2G_1 + G_2)}{m}\left(\frac{3}{2\pi}\right)^{3/2}\left(\frac{v}{a^3}\right) + O\left(\frac{v}{a^3}\right)^2 \tag{10}$$

The terms G_1, G_2, and G_3 are

$$G_n = (N - m + 1)^{-1} \sum_{j=1}^{N-m+1} \sum_{k>l} f_{kl}^{(n)} (k - l)^{-5/2} \tag{11}$$

$$n = 1, 2, 3$$

f_{kl} is shown in Table I along with a schematic representation of each of the G_n. In the diagrams shown in this table, the horizontal line refers to the polymer chain, whereas the curved line connects two portions of the chain which are interacting. The filled circles represent the internal portion of the chain for which the expansion factor is desired. Note that v/a^3 is assumed to be the same in eq 9 and 10. It can be seen from eq 9 and 10 and Table I that α_m involves additional sums G_1 and G_2 which do not appear in α. These terms involve interactions between chain segments other than the internal sequence of m monomers. If we are above but close to the Θ point, first-order perturbation theory is assumed to be valid and

Table I
Coefficients G_n in Equations 9 and 10

n	$f_{kl}^{(n)}$	range of k and l	schematic representation
1	$k - j$	$0 < l < j$ $j < k < j + m$	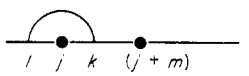
2	m	$0 < l < j$ $j + m < k < N$	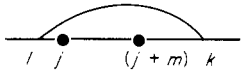
3	$k - l$	$j < l < k < j + m$	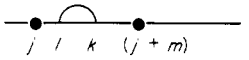

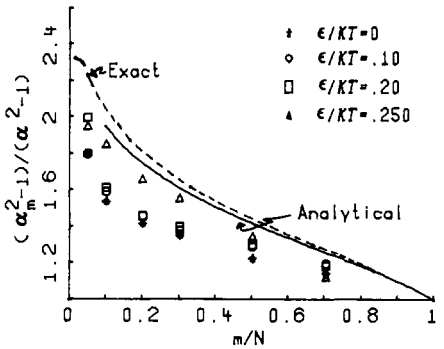

Figure 4. A comparison of the Monte Carlo and theoretical predictions of relative expansion of chains of 299 units, at various values of $\phi = \epsilon/kT$, as a function of internal sequence length. The theoretical predictions are based on first-order perturbation theory. The exact result is obtained from eq 11 and 12 and the analytical result from eq 13.

eq 9 and 10 can be combined to yield the ratio (setting $N = m$ in eq 9)

$$\frac{\alpha_m^2 - 1}{\alpha^2 - 1} = \frac{G_3 + 2G_1 + G_2}{G_3} \equiv 1 + F\left(\frac{m}{N}\right) \tag{12}$$

Note that α now refers to the end-to-end expansion factor for a chain of m units. $F(m/N)$ then represents the effect of the extra interactions on the internal chain conformation. This quantity is independent of temperature. The G functions in eq 11 can be summed numerically for finite N or can be evaluated analytically for large m and N. The analytical result for eq 12 can be obtained by integrating the equations by Chikahisa and Tanaka[12] to yield

$$F(\delta) = \frac{\delta^{-1/2}}{1 - \delta}\left\{\frac{32}{15\delta}[1 - (1 - \delta)^{5/2}] - \frac{16}{3} + \frac{5}{3}\delta^{1/2} + \delta + \frac{23}{15}\delta^{3/2} - \delta^2\right\} \tag{13}$$

$$N \gg 1 \qquad \delta = m/N > 0$$

The ratio in eq 12 was obtained from the Monte Carlo results and is plotted in Figure 4 for 299 unit chains. Also plotted in the figure is the exact result from eq 11 and the approximate analytical result, eq 13. It can be seen that perturbation theory is in qualitative agreement with the Monte Carlo calculations. As expected, the closest agreement is at $\phi = 0.250$ which is slightly above the estimated Θ point of $\phi = 0.28$. As the temperature is increased (or $\phi = \epsilon/kT$ decreased), the ratio F decreases for fixed δ. The reason for this decrease is probably the breakdown of first-order perturbation theory as one moves away from the Θ point.

It appears that the expansion of internal parts of the chain is responsible for the concave downward curves in Figure 4. This expansion of internal sequences of a chain has been pointed out before[11] and depends on the position

along the chain as well as the sequence length m. Furthermore, this effect does not disappear as $N \to \infty$. Thus one cannot rigorously equate the blob size ξ with the end-to-end distance of a chain of N_τ units as shown in eq 3, since the blob size itself depends upon the interactions between blobs. This interaction can be incorporated into the blob model by writing eq 12 as

$$\alpha_m^2 = \alpha^2 + (\alpha^2 - 1)F(m/N) \tag{14}$$

Where first-order perturbation theory applies, F can be found from eq 13. We can now write the blob size ξ_τ in eq 3, using eq 13 and perturbation theory

$$\xi_\tau^2 = N_\tau a^2\left\{1 + \left[1 + F\left(\frac{N_\tau}{N}\right)\right]\frac{4}{3}\left(\frac{3}{2\pi}\right)^{3/2}\left(\frac{v}{a^3}\right)N_\tau^{1/2} + ...\right\} \tag{15}$$

The mean square end-to-end distance then becomes

$$\langle r^2\rangle = a^2 N_\tau^{-1/5} N^{6/5} \times \left\{1 + \left[1 + F\left(\frac{N_\tau}{N}\right)\right]\frac{4}{3}\left(\frac{3}{2\pi}\right)^{3/2}\left(\frac{v}{a^3}\right)N_\tau^{1/2} + ...\right\} \tag{16}$$

If $F(N_\tau/N) = O(1)$, which is suggested by the Monte Carlo results in Figure 4 and eq 13, then the crossover behavior in eq 16 is essentially the same as the simple theory in eq 4 but modified by a temperature-dependent coefficient. In this modified blob model, the renormalization concept applies except that conformation within a blob is far from ideal.

Conclusions

We have used simulation data to illustrate the limitations of the blob approach to polymer statistics. Analysis of the internal configuration of the chain indicates that the simple blob concept employs an approximation which is inconsistent with the observed swelling of short chain segments. If the blob model is made more realistic, however, by incorporating the internal segment expansion effect as in eq 16, the predictions for overall chain dimensions are essentially proportional to the simplified theory in eq 4 for large N.

Comparison of the results obtained here with laboratory data on real systems suggests general agreement with some exceptions. Han and Akcasu,[13,14] for example, have analyzed large amounts of data on radius of gyration, diffusion, and viscosity and have found general agreement with the blob concept. This agreement, however, is not inconsistent with the conclusions drawn here since none of the data analyzed by Han and Akcasu are directly related to the properties of internal segments. The only direct experimental test of the blob concept is the neutron scattering experiments of Farnoux[1] et al. Their data are consistent with the blob concept but not with the results presented here. This discrepancy may be due to difficulties in the analysis of neutron data far out in the wings of the structure factor.

These simulations suggest that further analysis, both experimental and theoretical, is necessary before definitive conclusions can be reached on the single-chain problem. In particular, experimental data on the conformation of internal sequences would be very helpful. Such data could be obtained by small-angle neutron scattering if portions within a chain were deuterium tagged.

In the work presented here, perturbation theory was used to qualitatively show why internal portions of the chain would be expected to expand due to interactions with the rest of the chain. It should be pointed out, however, that there is evidence which suggests that conventional perturbation theory[2] is not completely correct since it does not include third- and higher order virial coefficients.[15-19] These higher order terms are thought to be significant in the region of the Θ point.

Acknowledgment. The authors acknowledge helpful discussions with Dr. Charles Han, at the National Bureau of Standards, which motivated us to use computer simulation techniques to investigate the "thermal blob" model. This work was supported by the U.S. Department of Energy under Contract DE-AC04-76 DP00789.

Appendix. Qualitative Dependence of $\langle r_m^2\rangle$ on m from Blob Theory

Blob theory can be generalized by allowing the configuration inside the blobs to be given by perturbation theory, considering the chain within the blob to be isolated. Thus for $m < N_\tau$ we can write to third order[2]

$$\alpha^2 = 1 + 1.333z - 2.075z^2 + 6.459z^3 + ... \tag{A1}$$

where the expansion parameter z is given by

$$z = \left(\frac{3}{2\pi}\right)^{3/2}\frac{v}{a^3}m^{1/2} \tag{A2}$$

with the binary cluster integral v defined in eq 8. The number of chain units per blob, N_τ, can now be defined as the maximum m for which eq A1 converges. This leads one to define N_τ approximately as[20]

$$N_\tau \sim (a^3/v)^2 \tag{A3}$$

This now allows us to write

$$\alpha^2 = 1 + 0.441\left(\frac{m}{N_\tau}\right)^{1/2} - 0.226\left(\frac{m}{N_\tau}\right) + 0.232\left(\frac{m}{N_\tau}\right)^{3/2} + ... \tag{A4}$$

$$\text{for } m/N_\tau < 1$$

For m larger than N_τ the blob theory assumes that the Flory mean field theory is valid.[2] This can also be written in terms of N_τ

$$\alpha^2 = (m/N_\tau)^{1/5} \tag{A5}$$

$$\text{for } m/N_\tau \gg 1$$

Equation A4 is plotted in Figure 2 for $m < 0.1N_\tau$, the estimated limit of the third-order perturbation theory. Likewise eq A5 is also plotted in Figure 2 for $m > 10N_\tau$. The intermediate range $0.1 < m/N_\tau < 10$ is uncertain since sufficient terms in eq A4 are not known and eq A5 is not valid near $m/N_\tau = 1$. We anticipate, however, that α^2 is a monotonic function of m/N_τ. This leads us to the conclusion that a plot of log α^2 vs. log (m/N_τ) should always be concave up to be consistent with the blob theory. In the intermediate range, the curve is schematically shown in Figure 2.

References and Notes

(1) B. Farnoux, F. Boue, J. P. Cotton, M. Daoud, G. Jannink, M. Nierlich, and P. G. de Gennes, *J. Phys. (Paris)*, **39**, 77 (1978).
(2) H. Yamakawa, "Modern Theory of Polymer Solutions", Harper and Row, New York, 1971.
(3) J. Mazur and F. L. McCrackin, *J. Chem. Phys.*, **49**, 648 (1968).
(4) F. L. McCrackin, M. Mazur, and C. M. Guttman, *Macromolecules*, **6**, 859 (1973).
(5) F. T. Wall and F. Mandel, *J. Chem. Phys.*, **63**, 4592 (1975).
(6) H. Okamoto, *J. Chem. Phys.*, **70**, 1690 (1979).
(7) F. T. Wall, F. Mandel, and J. Chin, *Proc. Natl. Acad. Sci. U.S.A.*, **76**, 2487 (1979).

(8) M. Metropolis, A. Rosenbluth, M. Rosenbluth, A. Teller, and E. Teller, *J. Chem. Phys.*, **21**, 1087 (1953).
(9) J. G. Curro, *J. Chem. Phys.*, **61**, 1203 (1974).
(10) F. T. Wall and W. A. Seitz, *J. Chem. Phys.*, **67**, 3722 (1977).
(11) M. Fixman, *J. Chem. Phys.*, **23**, 1656 (1955).
(12) Y. Chikahisa and T. Tanaka, *J. Polym. Sci., Part C*, **No. 30**, 105 (1970).
(13) A. Z. Akcasu and C. Han, *Macromolecules*, **12**, 276 (1979).
(14) C. Han and A. Z. Akcasu, to be published.
(15) P. G. de Gennes, *J. Phys. Lett. (Paris)*, **39**, L299 (1978).
(16) P. G. de Gennes, *J. Phys. Lett. (Paris)*, **36**, L55 (1975).
(17) Y. Oono and T. Oyama, *J. Phys. Soc. Jpn.*, **44**, 301 (1978).
(18) A. R. Khokhlov, *J. Phys. (Paris)*, **38**, 845 (1977).
(19) A. R. Khokhlov, *Polymer*, **19**, 1387 (1978).
(20) P. G. de Gennes, "Scaling Concepts in Polymer Physics", Cornell University Press, Ithaca, N.Y., 1979.

Functional Polymers in the Generation of Colloidal Dispersions of Amorphous Selenium

Thomas W. Smith* and Richard A. Cheatham

Xerox Corporation, Webster Research Center, Webster, New York 14580.
Received February 11, 1980

ABSTRACT: Stable colloidal dispersions of red, amorphous selenium have been prepared by the reduction of selenious acid in dilute aqueous solutions of hydrazonium polyacrylate. The initially formed particles average 1000–1200 Å in diameter. These particles can be grown by adding hydrazine and selenious acid in a cyclical fashion. Reduction of selenious acid in a control system in which hydrazonium propionate was substituted for the hydrazonium polyacrylate yielded a flocculent precipitate of amorphous selenium. The formation of the stable colloidal dispersion in the presence of the functional polymer can be understood in terms of a locus control formalism, which views the discrete polymer molecules as loci (submicroscopic reaction vessels) to which the reaction is restricted. Stable colloidal dispersions are then obtained because stabilization occurs in the same volume element in which the particle is nucleated. Hydrazonium salts of acrylic acid copolymers and other polyacids can also be utilized in the preparation of stable colloidal selenium dispersions.

Polymer-bound reagents and macromolecular catalysts have been extensively utilized in the synthesis of polypeptides,[1,2] catalysis of acyl transfer,[3] and numerous organic syntheses.[4–7] Most often, these reactions have involved functionalized, cross-linked, styrene–divinylbenzene resins. There are a few instances, however, where soluble macromolecules have been employed.[3,8] In this paper, we report the preparation of stable colloidal dispersions of red amorphous selenium with hydrazine, bound as hydrazonium ion, to soluble polyacids. The range of chemical processes for which macromolecular reagents are useful has thus been expanded to include the formation of colloidal sols.

Selenium has been of great importance as a photoconductive material.[9] Accordingly, it is useful to be able to prepare colloidal dispersions of elemental selenium and to control their particle size and size distribution.

Watillon and Dauchot[10] prepared monodisperse selenium particles by an elaborate procedure in which selenious acid was reduced in the presence of colloidal gold sols. The gold particles served as nuclei for the selenium particles. The resultant dispersions were quite dilute, having a volume fraction in selenium of 10^{-5}–10^{-6}.

The reduction of selenious acid with a functionalized polymer is a simple process through which fairly concentrated monodisperse selenium sols can be prepared. A typical dispersion is shown in Figure 1.

We have adopted the term locus control to describe our system in which functional macromolecules in solution act to generate a high concentration of insoluble atoms or molecules in their domain. At the submicron level, a locally supersaturated condition is thus created which effectively restricts particle nucleation to the domain of the polymer molecule. The idea of the locus control formalism is described in Scheme I. If one has a system in which there exists a uniform array of domains (soluble macromolecules, indicated by the circles) dispersed throughout a continuous medium in which there is dissolved a monomeric species M and if M will undergo a

Scheme I
The Locus Control Concept

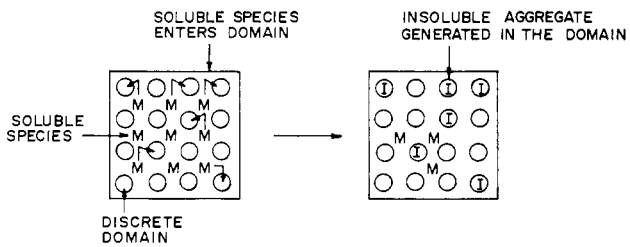

reaction leading to the formation of the aggregate insoluble species I in the domain but not in the continuous medium, then one has created a situation in which I must be generated in the locus of the domain. Just such a situation has been created through the binding of hydrazine, as hydrazonium ions, to the domain of polyacids. Thus, when selenious acid is added to a dilute aqueous solution of hydrazonium polyacrylate or hydrazonium polysulfonate, stable colloidal dispersions of red amorphous selenium are obtained. The polymer acts to control the particle size and number because selenium atoms are only generated in the domain of the polymer.

Experimental Section

A. Materials. Poly(acrylic acid) (Polysciences, Inc., mol wt 250 000, or K & K Laboratories, Inc., 2% aqueous solution) was used as received.

Copoly(styrene–acrylic acid) $(60/40)_M$ was prepared by the free-radical copolymerization of styrene (72.8 g, 0.70 mol) and acrylic acid (48.4 g, 0.70 mol). The polymerization was carried out for 18 h at 70 °C in ethyl acetate (480 mL) and was initiated with benzoyl peroxide (3.38 g, 0.014 mol). The monomers were reagent grade and inhibitors were removed chromatographically prior to polymerization. The polymerization was carried out under Ar in a stirred 1-L, four-necked flask. The reaction mixture was purged with N_2 for 1 h prior to initiation of the polymerization. The polymer was purified by reprecipitation from methanol into water. The acrylic acid content was determined to be 38.7 mol % by titration with 0.1 N sodium hydroxide.

0024-9297/80/2213-1203$01.00/0